Int J Clin Exp Pathol 2021;14(6):680-692
www.ijcep.com /ISSN:1936-2625/IJCEP0124940

Original Article

Uniformly-aligned gelatin/polycaprolactone fibers promote proliferation in adipose-derived stem cells and have distinct effects on cardiac cell differentiation

Dongying Zhang*, Kun Yu*, Xiao Hu, Aixia Jiang

*Department of Cardiology, The Affiliated Huaian No. 1 People's Hospital of Nanjing Medical University, Jiangsu, China. *Equal contributors.*

Received October 25, 2020; Accepted February 24, 2021; Epub June 15, 2021; Published June 30, 2021

Abstract: Cardiac tissue engineering is a promising technique to regenerate cardiac tissue and treat cardiovascular disease. Here we applied a modified method to generate ultrafine uniformly-aligned composite gelatin/polycaprolactone fibers that mimic functional heart tissue. We tested the physical properties of these fibers and analyzed how these composite fibrous scaffolds affected growth and cardiac lineage differentiation in rat adipose-derived stem cells (rADSCs). We found that uniformly aligned composite fiber scaffolds had an anisotropic arrangement, functional mechanical properties, and strong hydrophilicity. The anisotropic scaffolds improved cell attachment, viability, and proliferative capacity of ADSCs over randomly-aligned scaffolds. Furthermore, uniformly aligned composite fiber scaffolds increased the efficiency of cardiomyogenic differentiation, but might reduce the efficiency of cardiac conduction system cell differentiation in ADSCs compared to randomly-oriented scaffolds and tissue culture polystyrene. However, the randomly-oriented composite scaffolds showed no obviously facilitated effects over tissue culture polystyrene on the two cells' differentiation process. The above results indicate that the scaffold fiber alignment has a greater effect on cell differentiation than the composition of the scaffold. Together, the uniformly-aligned composite fibers displayed excellent physical and biocompatible properties, promoted ADSC proliferation, and played distinct roles in the differentiation of cardiomyogenic cells and cardiac conduction system cells from ADSCs. These results provide new insight for the application of anisotropic fibrous scaffolds in cardiac tissue engineering for both *in vitro* and *in vivo* research.

Keywords: Adipose-derived stem cell, randomly oriented scaffolds, uniformly aligned scaffolds, cardiomyogenic differentiation, cardiac conduction system cells

Introduction

Cardiovascular disease (CVD) is the leading cause of death of female patients in the UK [1]. In CVD, cardiomyocytes are lost in a process that is followed by tissue repair and remodeling, resulting in fibrosis and deterioration of the aligned myocardial tissue structure [2], thus affecting the contraction and electrical propagation of heart tissue. The tissue deterioration in CVD could be relieved by cardiac regeneration strategies, among which cardiac tissue engineering has been confirmed as a potential one [2]. Cardiac tissue engineering aims to mimic the native myocardium's cellular composition and architecture through constructing new tissue and assimilating the bioengineered donor tissue by the host milieu [3].

Cardiac tissue engineering requires seed cells, biomaterials, and scaffold fabrication methods [3]. Adipose-derived stem cells (ADSC) are widely used as seed cells in cardiac tissue engineering [3]. Upon stimulation, ADSCs can differentiate into several cardiac lineages, which can be used to restore deteriorated tissues [4], through decreasing infarction area, improving left ventricular function [5], or regenerating the cardiac conduction system (CCS) [6]. However, the main weakness of stem cell therapy is its low cell retention ratio in grafted tissue, which can be improved in tissue engineering when

combining cells with scaffolds using some fabrication methods [7]. Furthermore, in native heart tissues, cells and extracellular matrix (ECM) are anisotropically organized and often run parallel in specific directions. This anisotropic tissue architecture is a characteristic of heart muscle that could influence heart tissue structure and contractile strength [8]. To mimic natural cardiac tissue, fabricated scaffolds should resemble the anisotropic extracellular matrix (ECM), which can be recapitulated by electrospun nanofibers [9] through electrospinning methods. The nanofibrous scaffolds can be made of biocompatible materials [9, 10], which include natural polymers and synthetic polymers [3]. Gelatin (Gt), or denatured collagen, a natural polymer, and polycaprolactone (PCL), a synthetic polymer. Each have advantages and disadvantages in tissue engineering applications [11]. However, a Gt and PCL composite appears to offset the individual disadvantages of each and can generate an ECM with improved mechanical properties and favorable wettability [12].

Previous researches indicated that the anisotropic organization of fibrous scaffolds promoted mesenchymal stem cells (MSCs) differentiated into specific cell lineages [13, 14] based on the results using aligned PCL nanofibrous scaffolds. At the same time, the composition (collagen) of nanofibrous scaffolds could also affect stem cell fates, such as cell proliferation and differentiation [15]. Furthermore, the inherent morphologic and compositional inhomogeneity of the Gt/PCL composite [16] also affect the biologic properties of the fiber scaffold, which can be addressed using modified method and generated uniform and homogeneous nanofibers [16, 17]. However, the effects of utilizing this modified ultrafine uniform composite fibrous scaffold to engineer cardiac tissue remain unclear. Additionally, the influence of fiber alignment and composition on the differentiation of cardiomyocytes and other specialized CCS from ADSCs has not been tested.

In this study, we generated randomly-oriented and uniformly aligned electrospun nanofiber scaffolds using a modified method to mimic cardiac organization in failing and functional hearts [7]. We then investigated the physical properties of these fibrous scaffolds, the effects of tissue architecture on ADSC proliferation, and the differentiation processes of two specific cardiac cell types.

Material and methods

All experiments were performed following guidelines from the Animal Care and Experiment Committee of Nanjing Medical University.

Fabrication of randomly oriented and uniformly aligned Gt/PCL fiber scaffolds

Because the 50:50 weight ratio of Gt/PCL composites demonstrated well-developed physical properties and cell incorporation capabilities [18], we selected this weight ratio for the present study. Briefly, we dissolved a mixture composed of equal weights of Gt (Sigma-Aldrich, St Louis, MO, USA) and PCL (Sigma-Aldrich, St Louis, MO, USA) in acetic acid-doped trifluoroethanol (TFE) (0.2% relative to TFE) (Aladdin, Shanghai, China) at a concentration of 10% (weight:volume). The solution was subsequently loaded in a 10 ml syringe to generate randomly oriented nanofiber scaffolds. An appropriate amount of polyethylene oxide (PEO; molecular weight > 5,000,000 Da) (Sigma-Aldrich, St Louis, MO, USA) was added to the above solution to produce uniformly aligned nanofiber scaffolds [17].

A high-voltage power supply and a grounded static collector (Tongli Company, Shenzhen, China) were used to generate randomly-oriented nanofiber mats from the prepared Gt/PCL solution. The solution was dispensed into a 10 mL syringe and delivered by a 25-gauge blunt-tip needle at a 1.5 mL/h flow rate, using a programmable syringe pump. The voltage was set at 10 kV, and the distance between the syringe needle tip and the grounded collector was 15 cm.

For the uniformly aligned nanofiber scaffolds, a roller (Tongli Company, Shenzhen, China) was used to receive fibers instead of the stationary grounded collector. The conditions for the uniformly aligned nanofiber scaffold electrospinning were: syringe speed, 1.0 mL/h; voltage, 12 kV; and distance between the syringe needle tip and the grounded roller, 10 cm. All experiments were performed at room temperature with a relative humidity of 35-45%.

The electrospinning process lasted for 2 h, to generate randomly-oriented or uniformly-

aligned fiber mats with a thickness of 0.11-0.12 mm on cover slips that adhered to the aluminum foil collector. The resultant fiber mats were stored under a vacuum for 72 h to remove any residual solvent and then sterilized with ethanol and ultraviolet light for 30 min before cell seeding.

Microscopic morphology of randomly oriented and uniformly aligned fibrous scaffolds

Prior to the scanning electron microscopy (SEM) measurements, all samples were sputter-coated with gold for better conductivity, then we observed the morphology of the fibers with a scanning electron microscope (Leica, Cambridge Ltd, U.K.). We used Image J software to measure the fiber diameter from the SEM images and quantified the fiber diameters using the line tool to generate an intensity plot.

Mechanical properties measurement

We prepared randomly-oriented and uniformly-aligned fibrous scaffolds of about 0.5 mm thickness using the methods described in the previous section. We then cut the fibrous scaffolds into rectangular samples, 50 mm long and 10 mm wide. We measured thickness using an electronic meter at five different locations of each sample, and calculated the mean value. Unlike uniformly aligned scaffolds, the direction of measurement was not limited for randomly-oriented scaffolds, in which we measured fibers in both parallel and vertical directions. We performed the tensile test with a tensile test machine (Instron, Canton, MA, USA) and calculated the tensile strength, modulus of elasticity, and elongation at break based on the stress-strain relationship. The tensile rate of the instrument was set to 5 mm/min, and we tested at least 10 rectangular samples for each direction of fiber.

Measurement of static contact angle

After we generated randomly-oriented and uniformly-aligned fibrous scaffolds with smooth surface, as described in the first section, we loaded at least six pieces of each type on the static contact angle tester (Instron, Canton, MA, USA). We determined the static contact angle of each sample at 0 s, 10 s, 20 s, 30 s while 0.25 μL deionized water automatically dripped into the middle of the scaffold.

Isolation and culture of rat brown ADSCs

We isolated brown adipose-derived stromal cells from 1 to 2-day-old Sprague Dawley rats, according to the protocol by Planat-Bénard et al. [19]. We resuspended the resultant stromal vascular fraction (SVF) in PBS, counted cells by hemocytometer, and then plated at a density of 3×10^4 cells/cm^2 in Dulbecco's Modified Eagle's Medium (DMEM) supplemented with 10% fetal bovine serum (FBS) and 100 U/mL penicillin-streptomycin. The SVF cells were cultured at 37°C in a humidified atmosphere containing 5% CO_2 and subcultured when cells reached 80% confluence. After 3 weeks of culture, we seeded rat ADSCs (rADSCs) on randomly oriented or uniformly aligned electrospun scaffolds or on tissue culture polystyrene (TCP) in complete media to test the effects of scaffolds composition and alignment on cell behaviours.

Retention, viability, and proliferation of cultured ADSCs on fibrous scaffolds

To measure the retention ability of different fibrous scaffolds, we seeded the rADSCs on the scaffolds and on TCP at a density of 4,000 cells/cm^2. The adhesive rates of the fiber mats at 6 and 24 h were measured by subtracting the non-adhesive cell number from the total cell number and subsequently dividing by the total cell number.

We measured cell viability of rADSCs cultured on the two different scaffolds and TCP for 3 days and 5 days, using a Live/Dead assay kit (Life Technologies I, Carlsbad, CA 92008 USA), according to the manufacturer's instructions. We acquired images of selected areas using fluorescence microscopy and calculated cell viability by counting the number of live and dead cells using Image J software. Meanwhile, the effect of scaffolds composition and alignment on cell apoptosis were tested through TUNEL staining following the instructions of manufacturer (Abcam, Cambridge, UK).

The metabolic activity of ADSCs seeded on different fibrous scaffolds and TCP was determined using an Alamar Blue (AB) assay (Invitrogen, Grand Island, NY, USA) at 24 h, 3 days, 5 days, and 7 days of culture, according to the manufacturer's protocols. We measured

Table 1. Description of gene primers used in quantitative PCR

Gene	Primers	PCR product size
β-actin	5'-TCCTGCGTCTGGACCTGG-3'	159 bp
	5'-CCATCTCTTGCTCGAAGT-3'	
Gata-4	5'-CATGCTTGCAGTTGTGCTAG-3'	174 bp
	5'-ATTCTCTGCTACGGCCAGTA-3'	
α-SA	5'-GCTTCTATCATGCCTTCTCTGG-3'	118 bp
	5'-GCCAGCTTCTCATAGTCTTCC-3'	
cTnI	5'-TTGGTGTTGGATGGGCTG-3'	127 bp
	5'-TCTCAGTGATGTTCTTGGTGAC-3'	
Serca2α	5'-CAGCCATGGAGAACGCTCA-3'	128 bp
	5'-TCGTTGACCCCGAAGTGG-3'	
Gata6	5'-CTTGCGGGCTTTATATGAAACTC-3'	149 bp
	5'-GGAAGTTGGAGTCATAGGAACAG-3'	
Tbx3	5'-TGGTCATTACGAAGTCAGGAAG-3'	148 bp
	5'-ACCATCCACCGAGAATTGTG-3'	
Hcn4	5'-TCAGATGGCTCCTATTTTGGG-3'	119 bp
	5'-ACCTCGTTGAAGTTGTCCAC-3'	

fluorescent values for every sample in triplicate with a microplate reader (Biotek, USA).

Effects of fibrous scaffold composition and alignment on cardiac differentiation of rat brown ADSCs

Previous research suggested that rat brown ADSCs could differentiate into cardiomyocytes and CCS cells upon induction [6]. To test the effect of fibrous scaffold composition and alignment on cardiac cell differentiation, ADSCs were seeded on three different substrates: TCP, randomly-oriented, or uniformly-aligned nanofiber scaffolds. The three groups were all given 10 μmol/L 5-azacytidine (5-AZA) (Sigma-Aldrich, St Louis, MO, USA) to induce ADSCs for 24 h, then the medium was discarded and replaced with fresh total medium. After 3 weeks' culture, cells on the electrospun scaffolds or on TCP were proceeded for immunofluorescence staining or for reverse transcription quantitative polymerase chain reaction (RT-qPCR) to analyze the expression of cardiac lineage-specific markers.

Immunofluorescence staining assay

Cells grown on randomly-oriented or uniformly-aligned nanofiber scaffolds or on TCP were fixed in PBS containing 4% paraformaldehyde (PFA) for 30 min, then permeabilized with 2% Triton X-100 for 20 min, blocked with 5% bovine serum albumin (BSA) (Sigma-Aldrich, St. Louis, MO, USA) in PBS for 1 h at room temperature, and incubated with primary antibodies overnight. The primary antibodies were as follows: mouse monoclonal anti-BrdU (1:400; Sigma-Aldrich, St Louis, MO, USA), mouse monoclonal anti-α-actinin (sarcomeric) (1:400; Sigma-Aldrich, St Louis, MO, USA), rabbit polyclonal anti-troponin I (1:400; Abcam, Cambridge, UK), and mouse monoclonal anti-hyperpolarization-activated cyclic nucleotide-gated ion channels 4 (HCN4) (1:400; Abcam, Cambridge, UK). Cells were then washed three times for 5 min with PBS and stained with secondary antibodies, including Alexa Fluor 488- or Alexa Fluor 594-conjugated (1:1000; Abcam, Cambridge, UK) for 60 min at room temperature in the dark, and subsequently washed three times with PBS for 5 min. Nuclei were counterstained with 4,6-diamidino-2-phenylindole (DAPI) and fluorescent images were captured with a confocal microscope system (Leica, UK).

RNA isolation and RT-qPCR

We used RT-qPCR to compare the gene expression of several cardiac-specific markers involved in heart development in cells on different substrates. We isolated total RNA from cultured rADSCs on scaffolds or on TCP using RNeasy Mini Kit (Qiagen, Hilden, Germany) according to the protocol and quantified by spectrophotometry. We extracted circular DNA from 1 μg of total RNA using reverse transcription, following the manufacturer's protocols (Takara, Dalian, China). We quantified the RNA expression of cardiac-specific markers using RT-qPCR and SYBR dye with a C1000 CFX96 Real-Time System (Bio-Rad, USA). Cardiac-specific markers included GATA-binding factor 4 (GATA-4), sarcoplasmic reticulum Ca^{2+} ATPase 2a (SERCA2a), α-sarcomeric actinin (α-SA), cardiac troponin I (cTnI), T-box transcription factor 3 (Tbx3), GATA-binding factor 6 (GATA6), and hyperpolarization-activated cyclic nucleotide-gated ion channels 4 (HCN4). We used beta-actin as an endogenous reference gene and expression of beta-actin in the TCP group as a control. The primers for amplifying the above genes are listed in **Table 1**.

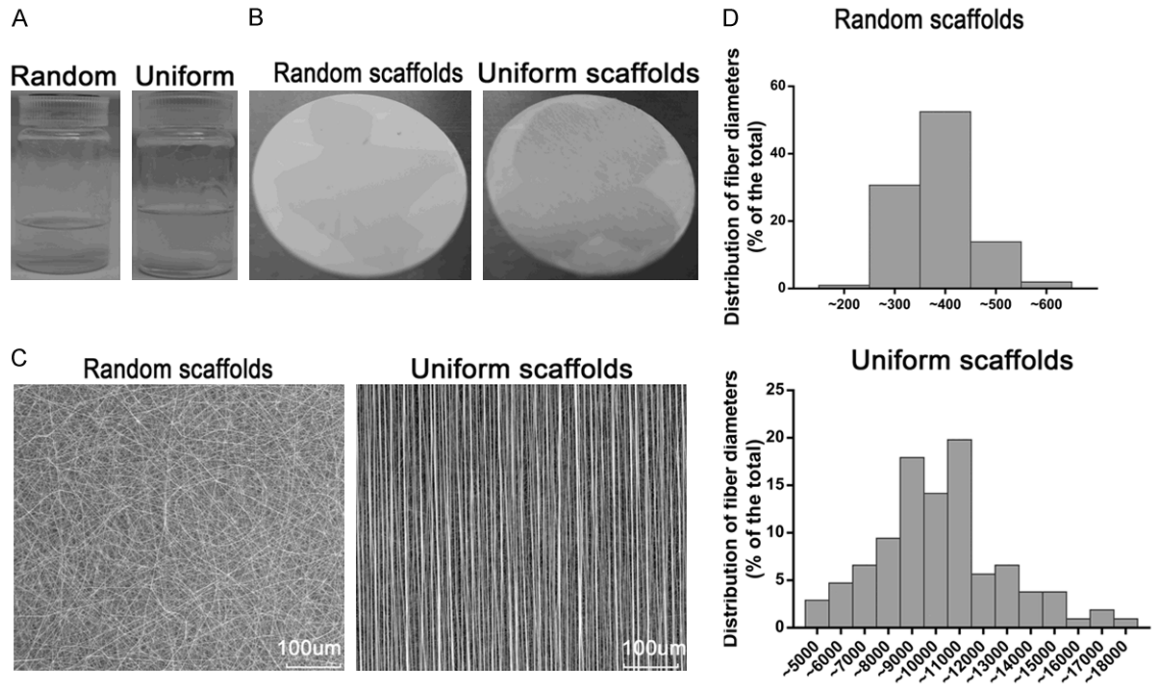

Figure 1. Fabrication and microscopic characterization of randomly-oriented and uniformly-aligned Gelatin/PCL fibrous scaffolds. A. The dissolving situations of the composite polymer prepared for the two aligned scaffolds. B. The appearance of randomly-oriented and uniformly-aligned fibrous scaffold. C. SEM micrographs of the two aligned fibrous scaffolds. D. The distribution of fiber diameters of the two aligned scaffolds (n = 200 from three independent samples). Random scaffolds = randomly-oriented fibrous scaffold, Uniform scaffolds = uniformly-aligned fibrous scaffold.

We used the following temperature protocol: 1 min at 95°C, 40 cycles of 10 s at 95°C and 30 s at 60°C, followed by 15 s at 95°C, 60 s at 60°C, and 15 s at 95°C.

Statistical analysis

All quantitative data are presented as mean ± standard deviation (SD). One-way ANOVA analysis followed by Tukey's post hoc test (GraphPad Prism 7.0) was performed to compare the differences among groups. Values of $P < 0.05$ were considered significant.

Results

Construction and microscopic characterization of electrospun fiber scaffolds

Three to five days after using the acetic acid-doping method as described above, the solution mixtures for generating randomly-oriented or uniformly-aligned scaffolds were clear and evenly dispersed, and the scaffold surfaces were smooth (**Figure 1A**, **1B**). Using SEM analysis, we confirmed that Gt/PCL fibrous meshes were uniformly homogeneous and had the desired random orientation or uniform alignment (**Figure 1C**). The diameters of the randomly-oriented and uniformly-aligned fibers were 330.07 ± 65.73 nm and 1580 ± 320 nm, respectively, with peak frequencies at 1000-1500 nm and 400-500 nm (**Figure 1D**).

Physical properties of randomly-oriented and uniformly-aligned scaffolds

As shown in **Figure 2A**, **2B**, the maximum tensile force (2.07 ± 0.42 N), tensile strength (6.51 ± 1.04 Mpa), Young's modulus (6.49 ± 1.42 Mpa), and fracture elongation rate (101.33 ± 8.0%) of the uniformly-aligned fibers in the longitudinal axis were higher than that of randomly-oriented fibers and uniformly-aligned fibers in the vertical axis. Compared to the randomly oriented scaffolds, the uniformly aligned scaffolds in the vertical axis had similar tensile strength, Young's modulus, and fracture elongation rate, but the maximum tensile strength was lower. The results indicated that aligned scaffolds in the longitudinal axis had advantag-

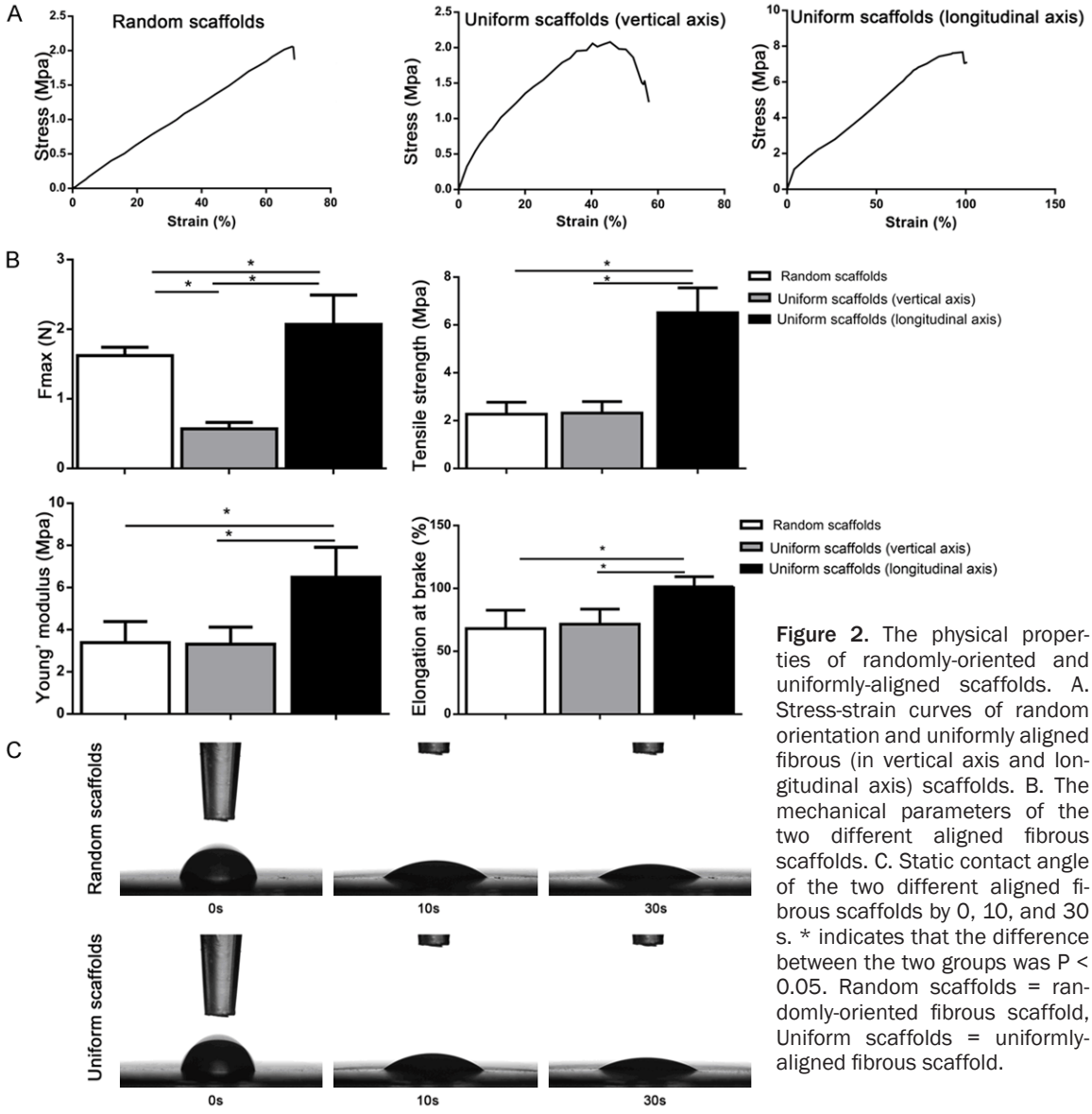

Figure 2. The physical properties of randomly-oriented and uniformly-aligned scaffolds. A. Stress-strain curves of random orientation and uniformly aligned fibrous (in vertical axis and longitudinal axis) scaffolds. B. The mechanical parameters of the two different aligned fibrous scaffolds. C. Static contact angle of the two different aligned fibrous scaffolds by 0, 10, and 30 s. * indicates that the difference between the two groups was $P < 0.05$. Random scaffolds = randomly-oriented fibrous scaffold, Uniform scaffolds = uniformly-aligned fibrous scaffold.

es in tension, rigidity, and elasticity properties, and thus possessed desirable mechanical properties for cardiac tissue engineering applications.

We measured the hydrophilicity of the random and aligned Gt/PCL fiber scaffolds using the static contact angle analysis. As shown in **Figure 2C**, the water contact angle was reduced to about 30° by 30 s, and the angle decreased to 0° by 51.08 ± 2.13 s and 48.66 ± 1.27 s in the randomly-oriented and uniformly-aligned scaffolds, respectively. There was no obvious difference in water contact angle between the two types of scaffolds ($P > 0.05$), indicating that the two kinds of fiber scaffolds were comparably hydrophilic.

Randomly-oriented and uniformly-aligned scaffolds possess strong cell adhesiveness and viability with rADSCs

After 6 h of culture, 95.67 ± 1.03% and 95.9 ± 0.95% of rADSCs had adhered to randomly-oriented and uniformly-aligned fiber scaffolds, respectively. This cell adhesion was slightly lower than that of the TCP group 98.88 ± 1.0%. Although the proportion of adhesive cells increased to 98.10 ± 0.46% in the random orientation scaffold and 99.2 ± 0.56% in the uniformly-aligned scaffold by 24 h of culture, we found no significant differences in cell adhesion between the three groups ($P > 0.05$) (**Figure 3A**).

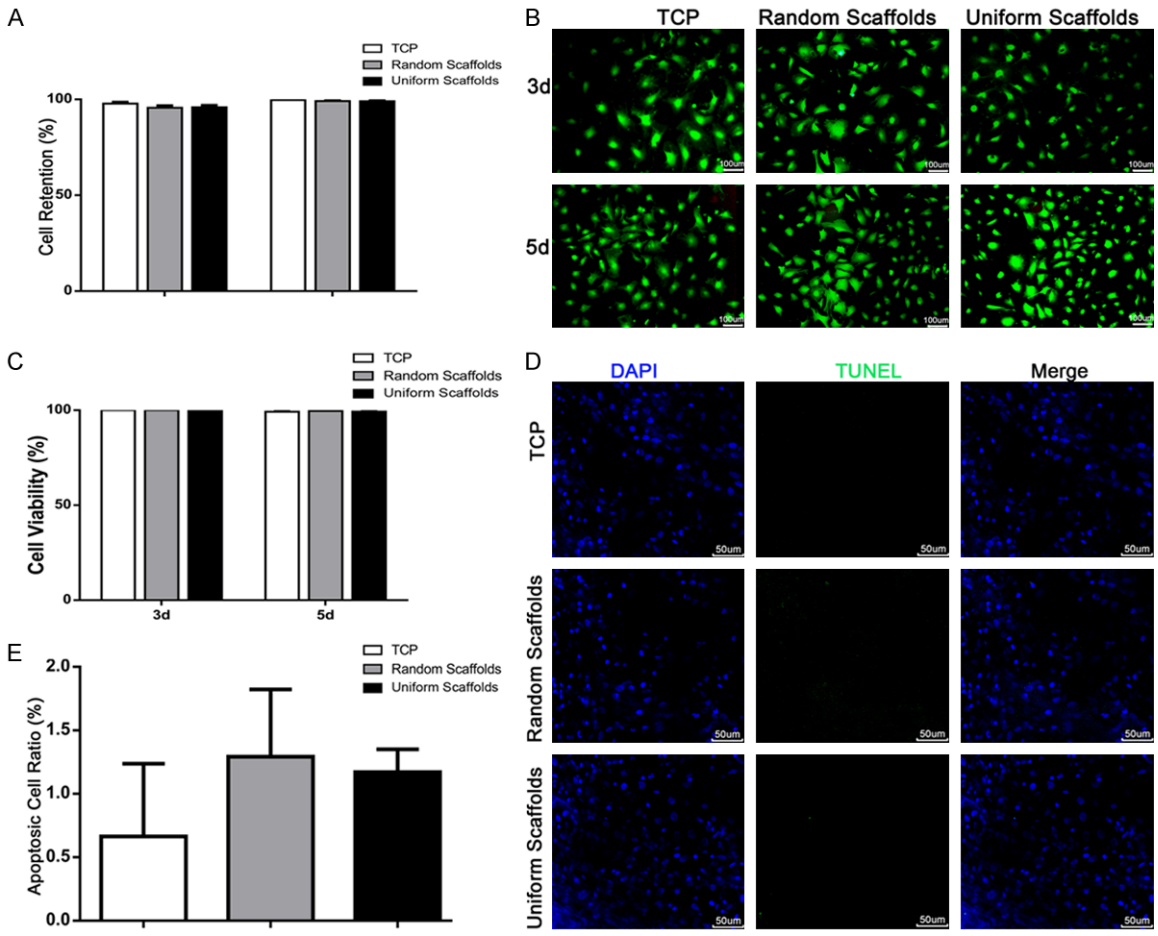

Figure 3. The biocompatibility of random orientation and uniformly aligned scaffolds with rADSCs. A. The adhesive ability of the two aligned fibrous scaffolds with rADSCs at 6 h and 24 h of culture, with cell culture plate as the control. B. Live/dead assay of rADSCs in the different groups after 3 days and 5 days of culture, in which the red fluorescent image represents dead cells and green represents living cells, bar = 100 um; C. Cell viability of the indicated groups as analyzed by calculating the ratio of living cells to total cells. Cells in five different random view fields were counted, with at least three samples for every group. D. Cell apoptosis assay of rADSCs in different groups after 5 days of culture, in which the green image represents apoptotic cells, bar = 75 um. E. Apoptotic cell ratio in different groups through calculating apoptotic cells versus the total cells. Random scaffolds = randomly-oriented fibrous scaffold, Uniform scaffolds = uniformly-aligned fibrous scaffold.

The rADSC viability results found that there were almost no dead cells in any of the three groups after 3 days of culture, and a slightly increased proportion of dead cells that indicated slightly decreased viability after 5 days of culture 99.80 ± 0.42% for TCP, 99.67 ± 0.58% for randomly oriented scaffolds, and 99.27 ± 0.64% for uniformly aligned scaffolds (**Figure 3B**, **3C**). We found no significant differences in cell viability between the two types of fiber scaffolds and TCP. Similar to the live/dead staining results, the apoptotic cell ratios in the three groups were quite low after 5 days' culture, 0.66 ± 0.57% for TCP, 1.29 ± 0.53% for randomly-oriented scaffolds, and 1.17 ± 0.17% for uniformly-aligned scaffolds respectively (**Figure 3D**, **3E**). Further analysis shown that there were no significant differences among the three groups in cell apoptosis. These results indicated that the composite scaffolds had no obvious toxic effects on rADSCs, and thus might be safely used for in vitro or in vivo research.

Uniformly-aligned fibers promote rADSC proliferation

The fluorescence values analyzed in the AB assay were almost equivalent by 24 h in the three groups; after 3 days, the fluorescence value stably increased in all groups. By days 5

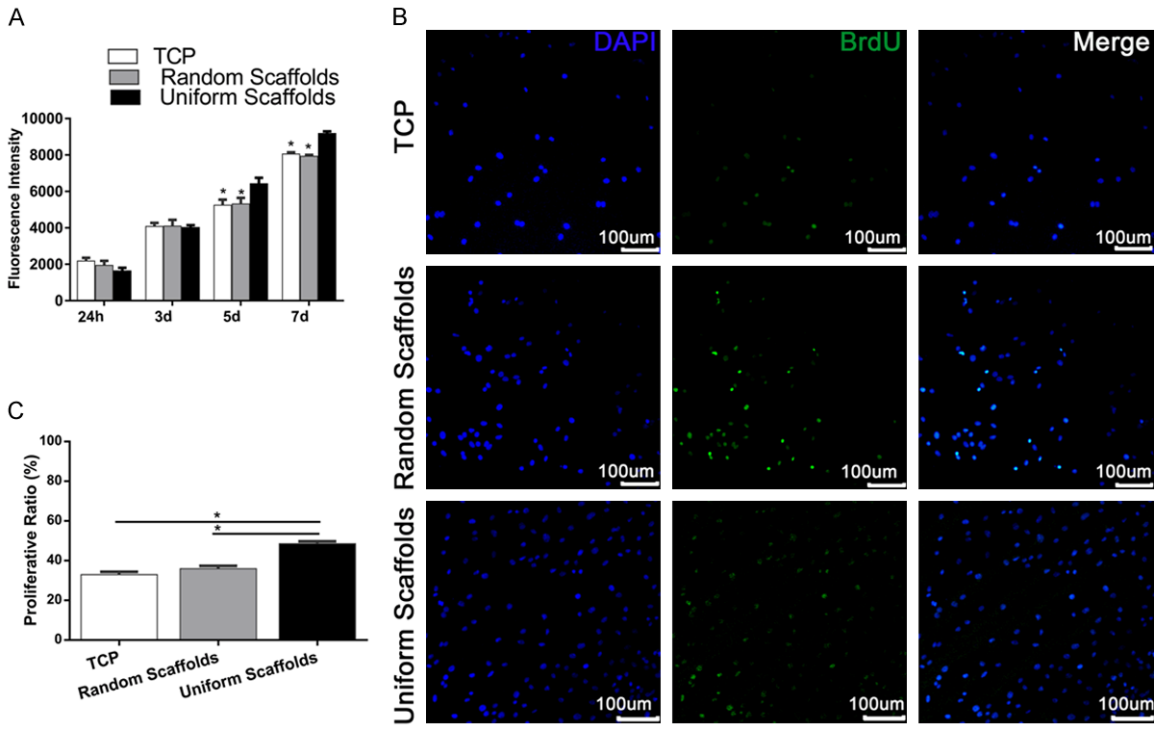

Figure 4. Proliferation of rADSCs on randomly-aligned and uniformly-aligned fibrous scaffolds, with cell culture plate as the control. A. Proliferative curve of rADSCs in the three groups analyzed by AB assay on days 1, 3, 5, and 7. B. BrdU immunofluorescence staining for rADSCs in different groups after 5 days of culture. Positive cells were stained green. C. Percentages of BrdU-positive rADSCs were calculated and compared under five different random view fields, with at least three samples for each group. * indicates that the difference when compared with the uniformly-aligned fibrous scaffold group was significant at $P < 0.05$. Random scaffolds = randomly-oriented fibrous scaffold, Uniform scaffolds = uniformly-aligned fibrous scaffold.

and 7, the values were significantly ($P < 0.05$) higher for the uniformly-aligned scaffold group than for the randomly-oriented scaffold and TCP groups (**Figure 4A**). However, for all the days, the fluorescence values were similar between the TCP and randomly oriented-scaffold group.

In order to verify the promotive effect of aligned orientation on rADSC proliferation, we measured the expression of the cell proliferation marker BrdU by immunofluorescence staining. As shown in **Figure 4B**, **4C**, after 5 days of culture, there were various degrees of cell proliferation in the three groups. The BrdU positive cell ratio was 48.57 ± 1.16% for the uniformly-aligned fiber scaffold, 35.97 ± 1.39% for the randomly-oriented fiber scaffold, and 32.98 ± 1.37% for the TCP group, suggesting that the uniformly-aligned fiber scaffold facilitated rADSC proliferation.

Taken together, our results indicated that the uniformly-aligned fiber scaffolds generated by our modified method might be safe and effective due to low cytotoxicity, promotion of cell proliferation, and strong cell adhesion capabilities. Thus, we determined that the uniformly-aligned Gt/PCL composite scaffolds were suitable for further use in in vitro and in vivo experiments.

Anisotropic orientation of scaffolds promotes cardiomyogenic differentiation of rADSCs

To examine the effect of scaffold fiber alignment on the differentiation efficiency of rADSCs into cardiomyocytes, we measured the expression of cardiac-specific genetic markers [19]. For the specific markers (Gata4, cTnI, Serca2a and α-SA), we found the expression in the uniformly-aligned group was higher than that in cells on randomly-oriented scaffolds after 3 week of culture ($P < 0.05$) (**Figure 5A**). For all four of the above genes, expression was slightly higher in cells on the randomly-oriented scaffolds than that on TCP, but there were no significant difference ($P > 0.05$).

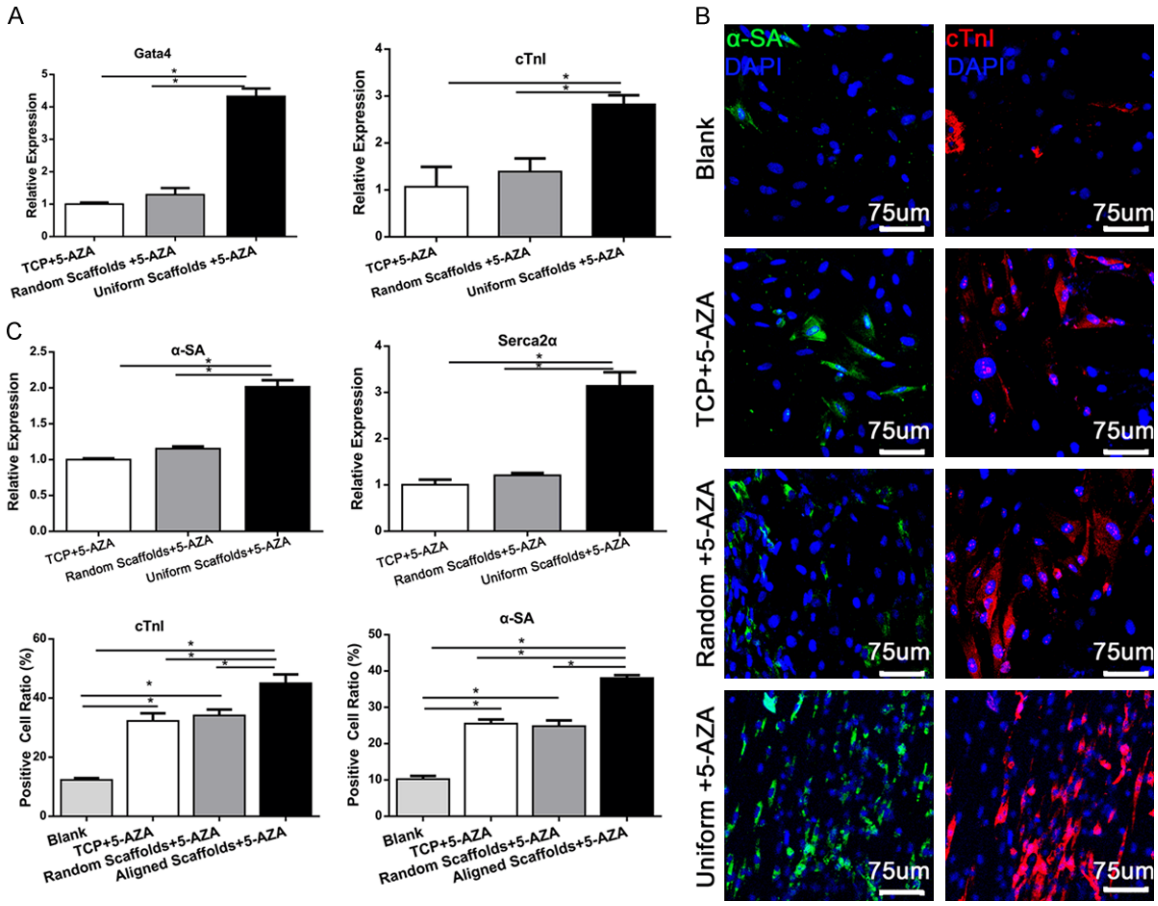

Figure 5. Effect of scaffold composition and architecture on cardiomyogenic differentiation from rADSCs. A. Relative expression of cardiac-specific markers (Gata4, α-SA, cTnI, and SERCA2α) after 3 weeks of incubation (n = 3). B. Confocal microscopy images of troponin-I (red) and α-SA (green) in cells of the indicated groups after 3 weeks of culture. C. Percentages of cTnI and α-SA-positive rADSCs were calculated and compared under five different random view fields, with least three samples for each group. * indicates the difference between the two groups was $P < 0.05$. Random or Random scaffolds = randomly-oriented fibrous scaffold, Uniform or Uniform scaffolds = uniformly-aligned fibrous scaffold.

In order to test the effect of uniformly aligned fiber organization on the differentiation of adipose stem cells into cardiomyocytes, we measured the expression of cardiomyocyte-specific markers, cTnI and α-SA. For this experiment, we used immunofluorescence staining of the three groups after 3 weeks induction by 5-AZA, and used cells cultured in TCP without 5-AZA induction as the control (blank). As shown in **Figure 5B**, **5C**, rADSCs seldom spontaneously differentiated into cTnI and α-SA positive cells. With 5-AZA induction, the ratio of cTnI and α-SA positive cells increased in all groups. With both 5-AZA induction and uniformly aligned fibers, the proportion further increased. The percentage of cTnI-positive cells in the uniformly-aligned fiber scaffold group (45.03 ± 3%) was higher than that of the randomly-oriented fiber scaffold group (34.12 ± 1.99%) and the TCP group (32.27 ± 2.6%). Similar to cTnI expression, the percentage of α-SA-positive cells was higher in the uniformly-aligned fiber scaffold group (38.06 ± 0.81%) than in the randomly-oriented fiber scaffold group (24.8 ± 1.6%) or in the TCP group (25.5 ± 1.14%). Taken together, these results suggest that the uniformly-aligned fiber organization promotes cardiomyogenic differentiation from ADSCs.

Inhibitory effect of anisotropic scaffold orientation on CCS cell differentiation from rADSCs

CCS cells are another functional cardiac cell type that are predominantly differentiated from precursor myocytes [20], but their differentiation process can be inversely inhibited [21],

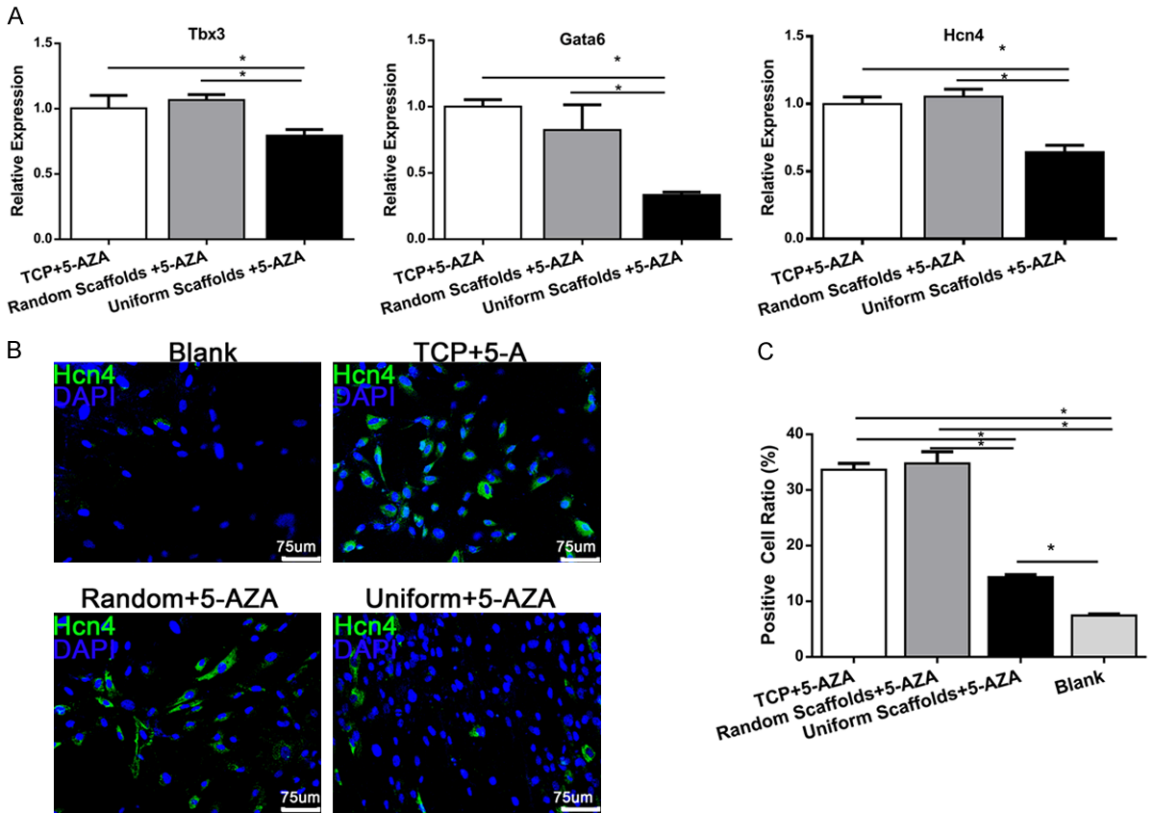

Figure 6. Effects of fiber composition and alignment on CCS cell differentiation from rADSCs. A. Relative expression of CCS-specific markers Gata6, Tbx3, and Hcn4 at 3 weeks after induction. B-actin expression was used in the TCP group as an internal control. B. Confocal microscopy images of Hcn4 expression (green) in cells of the indicated groups after 3 weeks of culture. C. Percentages of HCN4-positive rADSCs were calculated and compared under five different random view fields, with at least three samples for each group. * indicates the difference between the two groups was significant at $P < 0.05$. Random or Random scaffolds = randomly-oriented fibrous scaffold, Uniform or Uniform scaffolds = uniformly-aligned fibrous scaffold.

indicating that CCS and cardiomyogenic differentiation processes are regulated in different ways. However, the effect of anisotropic tissue architecture on CCS cell differentiation remains unclear.

We found that the gene expression of three CCS specific markers: hyperpolarization-activated cyclic nucleotide-gated ion channels 4 (HCN4), GATA-binding factor 6 (GATA6), and T-box transcription factor 3 (Tbx3) [6] were similar in cells cultured on TCP and on randomly-oriented scaffolds. However, the expression of Tbx3, a novel and specific marker of the CCS [22-24], was significantly lower in cells seeded on the uniformly-aligned scaffolds than in the randomly-oriented scaffold group and the TCP group ($P < 0.05$). Similarly, we found that other CCS marker expression GATA6 [25, 26] and HCN4 [27] was also significantly downregulated in cells on uniformly-aligned scaffolds compared to those on randomly-oriented scaffolds and those in the TCP group ($P < 0.05$) (**Figure 6A**).

As seen in **Figure 6B**, **6C**, rADSCs seldom spontaneously differentiated into HCN4-positive expression cells. With 5-AZA induction, the ratio of HCN4-positive cells significantly increased ($P < 0.05$); however, the proportion of HCN4-positive cells may decrease with a uniformly aligned fiber organization. The frequencies of HCN4-positive cells were 33.64 ± 1.13% in TCP group, 34.78 ± 2.12% in the randomly-oriented fiber scaffold group, and 14.35 ± 0.42% in the uniformly-aligned fiber scaffold group. The ratio of HCN4-positive cells in the uniformly-aligned fiber scaffold group was lower than that of the TCP and randomly-oriented fiber scaffold groups. Taken together, these

results suggest that anisotropic tissue architecture may inhibit CCS cell differentiation from ADSCs.

Discussion

Using the new modified methods to alleviate the inhomogeneity of composite polymers, we generated ultrafine uniformly-aligned fiber scaffolds and scaffolds with randomly-oriented fibers. Our research showed that uniformly-aligned fiber scaffolds effectively mimicked the mechanical properties of natural myocardium [28], and thus could give mechanical support for in vivo or in vitro experiments. Additionally, both uniformly aligned and randomly oriented scaffolds were strongly hydrophilic, a property which facilitates cell adhesion and growth onto the scaffolds [29]. Furthermore, the biocompatibility of uniformly-aligned scaffolds with rADSCs showed that uniformly-aligned scaffolds have improved cell adhesion capabilities, were nearly non-cytotoxic, and promoted cell proliferation, supporting the further use of this type of scaffold for in vitro experiments.

Several studies suggested that the stem cell differentiation efficiency could be enhanced by using elastic chemical compounds, such as gelatin [30] or laminin [31], and be further enhanced by combining elastic compounds with three-dimensional supports that would serve as microcarriers [32]. Other factors in tissue engineering also involved in the stem cell differentiation process. Uniformly-aligned fiber scaffolds facilitate the differentiation of human pluripotent stem cell-derived cardiomyocytes (hPSC-CM) [33] and the differentiation of cardiomyocytes from ADSCs [14]. In the earlier stage of our experiment, we tried to investigate the effect of scaffold fiber alignment on cardiomyogenic differentiation from rADSCs without 5-AZA induction; however, possibly due to the low spontaneous differentiation efficiency, we did not observe positive results. With 5-AZA induction, the differentiation efficiency was increased in the TCP, randomly-oriented, and uniformly-aligned fiber scaffold groups. Furthermore, our research showed that use of a uniformly-aligned composite Gt/PCL fiber scaffolds further increased the gene and protein expression of cardiac-specific markers. This study demonstrated that a uniformly-aligned fiber orientation enhanced the cardiomyogenic differentiation from rADSCs, and that randomly-oriented scaffolds generated from the gelatin-containing composite did not show an advantage over conventional TCP. These results indicate that the scaffold fiber alignment has a greater effect on cell differentiation than the composition of the scaffold.

CCS cells are another functionally distinct heart muscle type that initiate, propagate, and coordinate the electric impulse. Recent studies confirmed that cells in peripheral and central conduction tissues are derived from cardiomyogenic progenitors, rather than migratory neuroectoderm-derived populations [34]. Additionally, these cells were found to be inversely influenced by the cardiomyogenic differentiation process [21]. Takahashi et al found that brown adipose-derived stem cells could differentiate into cardiomyocyte and CCS cells, by analyzing the expression of markers specific to these two cell types [6]. By assessing the expression of three CCSs-specific markers [6, 35-37], we confirmed that rat brown adipose-derived stem cells also differentiated into CCS cells, but found that the frequency of spontaneous differentiation was quite low. However, the differentiation efficiency was increased with 5-AZA in all groups. Interestingly, a uniformly-aligned fiber orientation downregulated the CCS cell differentiation, as evidenced by significantly decreased expression of CCS-specific markers HCN4, Gata6, and Tbx3 in the uniformly-aligned scaffold group. This conclusion was further supported by a lower frequency of HCN4-positive cells on uniformly-aligned scaffolds than on TCP or on randomly-oriented scaffolds. Taking the findings of this study together, we hypothesize that anisotropic tissue organization inhibits CCS cell differentiation from rADSCs and that the use of uniformly-aligned fiber scaffolds in cardiac tissue engineering may decrease the arrhythmia occurrence rate associated with stem cell therapy, and thus have practical meaning in cardiac tissue engineering. However, the mechanism underlying the effect of cardiac tissue anisotropy on cardiac tissue differentiation is unknown, possibly through the cell matrix signaling pathways [8], which should be considered in future studies.

Conclusion

This study demonstrated that our technique to generate ultrafine randomly-oriented and uni-

formly-aligned fibrous scaffolds can mimic the failing and functional cardiac tissue ECM. The uniformly-aligned fiber scaffolds possessed the desired mechanical properties and hydrophilicity. Additionally, when used with rADSCs, the uniformly-aligned scaffolds had high cell retention, facilitated cell proliferation, and had nearly non-cytotoxic properties. Further, we found that the rADSCs spontaneously differentiated into cardiomyocytes and CCS cells, and that 5-AZA treatment increased the differentiation efficiency. Moreover, the uniformly-aligned fiber organization facilitated cardiomyogenic differentiation from rADSCs, but may have inhibited CCS cell differentiation. Further studies will be required to characterize the underlying mechanism of the effects of scaffolding type on these two cardiac cell differentiation processes.

Disclosure of conflict of interest

None.

Abbreviations

NRVCMs, neonatal rat ventricular cardiomyocytes; ADSCs, adipose-derived stem cells; ECM, extracellular matrix; Gt, gelatin; PCL, polycaprolactone; CCS, cardiac conduction system; TCP, tissue culture polystyrene; α-SA, α-sarcomeric actinin; SERCA2α, sarcoplasmic reticulum Ca2+ ATPase 2α; 5-AZA, 5-azacytidine; SEM, Scanning Electron Microscopy; DAPI, 4,6-diamidino-2-phenylindole; Tbx3, T-box transcription factor 3; HCN4, hyperpolarization-activated cyclic nucleotide-gated ion channels 4.

Address correspondence to: Dr. Aixia Jiang, Department of Cardiology, The Affiliated Huaian No. 1 People's Hospital of Nanjing Medical University, Huaian 223300, Jiangsu, China. Tel: +86-137-7047-5661; Fax: +86-0517-8087-8604; E-mail: hayyjax@njmu.edu.cn

References

[1] Bhatnagar P, Wickramasinghe K, Williams J, Rayner M and Townsend N. The epidemiology of cardiovascular disease in the UK 2014. Heart 2015; 101: 1182-1189.

[2] Liau B, Zhang D and Bursac N. Functional cardiac tissue engineering. Regen Med 2012; 7: 187-206.

[3] Georgiadis V, Knight RA, Jayasinghe SN and Stephanou A. Cardiac tissue engineering: renewing the arsenal for the battle against heart disease. Integr Biol (Camb) 2014; 6: 111-126.

[4] Planat-Benard V, Menard C, Andre M, Puceat M, Perez A, Garcia-Verdugo JM, Penicaud L and Casteilla L. Spontaneous cardiomyocyte differentiation from adipose tissue stroma cells. Circ Res 2004; 94: 223-229.

[5] Guan J, Wang F, Li Z, Chen J, Guo X, Liao J and Moldovan NI. The stimulation of the cardiac differentiation of mesenchymal stem cells in tissue constructs that mimic myocardium structure and biomechanics. Biomaterials 2011; 32: 5568-5580.

[6] Takahashi T, Nagai T, Kanda M, Liu ML, Kondo N, Naito AT, Ogura T, Nakaya H, Lee JK, Komuro I and Kobayashi Y. Regeneration of the cardiac conduction system by adipose tissue-derived stem cells. Circ J 2015; 79: 2703-2712.

[7] Rath R, Lee JB, Tran TL, Lenihan SF, Galindo CL, Su YR, Absi T, Bellan LM, Sawyer DB and Sung HJ. Biomimetic microstructure morphology in electrospun fiber mats is critical for maintaining healthy cardiomyocyte phenotype. Cell Mol Bioeng 2016; 9: 107-115.

[8] Tandon V, Zhang B, Radisic M and Murthy SK. Generation of tissue constructs for cardiovascular regenerative medicine: from cell procurement to scaffold design. Biotechnol Adv 2013; 31: 722-735.

[9] Barnes CP, Sell SA, Boland ED, Simpson DG and Bowlin GL. Nanofiber technology: designing the next generation of tissue engineering scaffolds. Adv Drug Deliv Rev 2007; 59: 1413-1433.

[10] Jawad H, Lyon AR, Harding SE, Ali NN and Boccaccini AR. Myocardial tissue engineering. Br Med Bull 2008; 87: 31-47.

[11] Pok S and Jacot JG. Biomaterials advances in patches for congenital heart defect repair. J Cardiovasc Transl Res 2011; 4: 646-654.

[12] Zhang Y, Ouyang H, Lim CT, Ramakrishna S and Huang ZM. Electrospinning of gelatin fibers and gelatin/PCL composite fibrous scaffolds. J Biomed Mater Res B Appl Biomater 2005; 72: 156-165.

[13] Lim SH and Mao HQ. Electrospun scaffolds for stem cell engineering. Adv Drug Deliv Rev 2009; 61: 1084-1096.

[14] Safaeijavan R, Soleimani M, Divsalar A, Eidi A and Ardeshirylajimi A. Comparison of random and aligned PCL nanofibrous electrospun scaffolds on cardiomyocyte differentiation of human adipose-derived stem cells. Iran J Basic Med Sci 2014; 17: 903-911.

[15] Shih YR, Chen CN, Tsai SW, Wang YJ and Lee OK. Growth of mesenchymal stem cells on electrospun type I collagen nanofibers. Stem Cells 2006; 24: 2391-2397.

[16] Feng B, Duan H, Fu W, Cao Y, Jie Zhang W and Zhang Y. Effect of inhomogeneity of the electrospun fibrous scaffolds of gelatin/polycaprolactone hybrid on cell proliferation. J Biomed Mater Res A 2015; 103: 431-438.
[17] Wang W, He J, Feng B, Zhang Z, Zhang W, Zhou G, Cao Y, Fu W and Liu W. Aligned nanofibers direct human dermal fibroblasts to tenogenic phenotype in vitro and enhance tendon regeneration in vivo. Nanomedicine (Lond) 2016; 11: 1055-72.
[18] Feng B, Tu H, Yuan H, Peng H and Zhang Y. Acetic-acid-mediated miscibility toward electrospinning homogeneous composite nanofibers of GT/PCL. Biomacromolecules 2012; 13: 3917-3925.
[19] Suzuki E, Fujita D, Takahashi M, Oba S and Nishimatsu H. Adipose tissue-derived stem cells as a therapeutic tool for cardiovascular disease. World J Cardiol 2015; 7: 454-465.
[20] Mikawa T and Hurtado R. Development of the cardiac conduction system. Semin Cell Dev Biol 2007; 18: 90-100.
[21] Christoffels VM, Smits GJ, Kispert A and Moorman AF. Development of the pacemaker tissues of the heart. Circ Res 2010; 106: 240-254.
[22] Hoogaars WM, Tessari A, Moorman AF, de Boer PA, Hagoort J, Soufan AT, Campione M and Christoffels VM. The transcriptional repressor Tbx3 delineates the developing central conduction system of the heart. Cardiovasc Res 2004; 62: 489-499.
[23] Hoogaars WM, Engel A, Brons JF, Verkerk AO, de Lange FJ, Wong LY, Bakker ML, Clout DE, Wakker V, Barnett P, Ravesloot JH, Moorman AF, Verheijck EE and Christoffels VM. Tbx3 controls the sinoatrial node gene program and imposes pacemaker function on the atria. Genes Dev 2007; 21: 1098-1112.
[24] Bakker ML, Boukens BJ, Mommersteeg MT, Brons JF, Wakker V, Moorman AF and Christoffels VM. Transcription factor Tbx3 is required for the specification of the atrioventricular conduction system. Circ Res 2008; 102: 1340-1349.
[25] Liu F, Lu MM, Patel NN, Schillinger KJ, Wang T and Patel VV. GATA-binding factor 6 contributes to atrioventricular node development and function. Circ Cardiovasc Genet 2015; 8: 284-293.
[26] Davis D, Edwards A, Juraszek A, Phelps A, Wessels A and Burch J. A GATA-6 gene heart-region-specific enhancer provides a novel means to mark and probe a discrete component of the mouse cardiac conduction system. Mech Dev 2001; 108: 105-119.
[27] Herrmann S, Layh B and Ludwig A. Novel insights into the distribution of cardiac HCN channels: an expression study in the mouse heart. J Mol Cell Cardiol 2011; 51: 997-1006.
[28] Engelmayr G, Cheng M, Bettinger C, Borenstein J, Langer R and Freed L. Accordion-like honeycombs for tissue engineering of cardiac anisotropy. Nat Mater 2008; 7: 1003-1010.
[29] Oh SH and Lee JH. Hydrophilization of synthetic biodegradable polymer scaffolds for improved cell/tissue compatibility. Biomed Mater 2013; 8: 014101.
[30] Obara C, Takizawa K, Tomiyama K, Hazawa M, Saotome-Nakamura A, Gotoh T, Yasuda T and Tajima K. Differentiation and molecular properties of mesenchymal stem cells derived from murine induced pluripotent stem cells derived on gelatin or collagen. Stem Cells International 2016; 2016: 1-10.
[31] van Dijk A, Niessen HW, Zandieh Doulabi B, Visser FC and van Milligen FJ. Differentiation of human adipose-derived stem cells towards cardiomyocytes is facilitated by laminin. Cell Tissue Res 2008; 334: 457-467.
[32] Karam JP, Bonafe F, Sindji L, Muscari C and Montero-Menei CN. Adipose-derived stem cell adhesion on laminin-coated microcarriers improves commitment toward the cardiomyogenic lineage. J Biomed Mater Res A 2015; 103: 1828-1839.
[33] Han J, Wu Q, Xia Y, Wagner MB and Xu C. Cell alignment induced by anisotropic electrospun fibrous scaffolds alone has limited effect on cardiomyocyte maturation. Stem Cell Res 2016; 16: 740-750.
[34] Cheng G, Litchenberg WH, Cole GJ, Mikawa T, Thompson RP and Gourdie RG. Development of the cardiac conduction system involves recruitment within a multipotent cardiomyogenic lineage. Development 1999; 126: 5041-5049.
[35] Wiese C, Nikolova T, Zahanich I, Sulzbacher S, Fuchs J, Yamanaka S, Graf E, Ravens U, Boheler KR and Wobus AM. Differentiation induction of mouse embryonic stem cells into sinus node-like cells by suramin. Int J Cardiol 2011; 147: 95-111.
[36] Yang J, Song T, Wu P, Chen Y, Fan X, Chen H, Zhang J and Huang C. Differentiation potential of human mesenchymal stem cells derived from adipose tissue and bone marrow to sinus node-like cells. Mol Med Rep 2012; 5: 108-113.
[37] Tsai SY, Chen S and Evans T. Efficient generation of cardiac purkinje cells from ESCs by activating cAMP signaling. Stem Cell Reports 2015; 4: 1089-1102.